EXPERIMENTAL INVESTIGATION OF DESIGN PARAMETERS IN AN IMPINGEMENT STARTING SYSTEM FOR TURBOSHAFT ENGINES

N. Kuen, L. Stecher Alonso Lillo, C. Helcig, V. Gümmer
Technical University of Munich (TUM), Department of Aerospace and Geodesy, Chair of Turbomachinery and Flight Propulsion, Garching b. München, Germany

Abstract

This paper investigates the influence of different design parameters of a pneumatic system used to spin-up the gas generator of a helicopter turboshaft gas turbine. The system uses supersonic nozzles to impinge air on the outer section of the compressor's radial end-stage. After identifying the relevant variables, Design of Experiments is used to vary and investigate their effects on the performance systematically and to discover possible interactions. The results of static experiments show good accordance with analytical calculations, however, acceleration experiments revealed interesting non-linear effects. The nozzle exit Mach number was identified as the most critical parameter. The Mach number is linked with the supply pressure and is, therefore, the reason for a design conflict. Prediction models are derived to get a data base for the redesign of the impingement system.

Keywords

experimental, design of experiments, impingement nozzle

NOMENCLATURE

Latin Symbols

A	cross sectional area	m^2
C_d	nozzle discharge coefficient	-
F	force	N
l	lever length	m
$\dot{m}$	mass flow rate	$\mathrm{kg/s}$
Ma	Mach number	-
$p,\ p_t$	pressure, total pressure	Pa
R	specific gas constant	$\mathrm{J/(kg\,K)}$
r	nozzle installation radius	m
$T,\ T_t$	temperature, total temperature	K
u	measurement uncertainty	
v	velocity	$\mathrm{m/s}$
Z	compressibility factor	-

Greek Symbols

α	nozzle installation angle	deg
η	impingement efficiency	-
γ	ratio of specific heats	-
μ	sample mean	
σ	sample standard deviation	
τ	shaft torque	N m

Indices

$crit$	critical
des	design
eff	effective
ex	nozzle exit
id	ideal
imp	impingement
in	nozzle inlet
red	reduced
th	nozzle throat

Abbrevations

ANOVA	Analysis of Variance
CCD	Central Composite Design
DOE	Design of Experiments
QSS	Quick-Start System

doi: 10.25967/550175

1. INTRODUCTION

The start of a rotorcraft requires high power which is often supplied by multiple engines. In cruise flight, the power demand is lower compared to the start condition. Therefore, it would be possible to save fuel, lower emissions and increase the range of the flight vehicle merely by switching off unnecessary engines. In any situation, the engine power needs to be ready on demand. The flight idle start-up time of a turboshaft engine can be found in order of seconds up to minutes, depending on the starting system. One possibility of a rapid start system is pressurized air impinging on the radial compressor wheel and using the momentum delivered by supersonic air to accelerate the gas generator.

Air turbine starters are commonly used as regular starting systems for gas turbines, especially of large-sized engines. However, the principle is different from an impingement starting system since air turbines use the aerodynamics of the turbine airfoils. Impingement on compressor or turbine impellers is a technique for spinning-up turbochargers in situations where not enough exhaust gas from the internal combustion engine is available.

First notes on the use of this technology are given in a patent by Garve [1]. The influence of the installation angle of the impingement channels is mentioned. More detailed information can be found in the patents of Schröder *et al*. [2] and Legg [3]. Both give more detailed information about nozzle counts, exact impingement location and the installation angle ranging from $15\,\mathrm{deg}$ to $25\,\mathrm{deg}$. Both sources refer to the possibility of applying different geometries for the impingement channels which seem to be straight drill holes. Since these systems are used in applications where size and weight do not matter, many impingement channels are used and the amount of impingement air is no design criterium. Daggett [4] describes a turbine impingement starting system for large aircraft engines as a lightweight alternative to standard starter devices. However, for this design minimizing the starting time is not of interest, neither is the amount of impingement air since it is supplied from a ground unit or with bleed air.

Veilleux [5] refers to a similar system for an application in a rotorcraft but without the rapid-start capability. The nozzle system can be applied to an axial or radial compressor as well as a turbine wheel. It has no internal air storage but a power source that supplies the nozzles with pressurized air. No detailed information about the design of the nozzles is given but the power source's pressure level of $276\,\mathrm{kPa}$ suggests that supersonic nozzles are used. Jones [6] mentions a rapid start system for small turbojets for application in military drones and missiles. It uses oxygen from a high-pressure reservoir which a pressure regulator then reduces to about $34.5\,\mathrm{bar}$. The system is designed to spin the engine up to $80{,}000\,\mathrm{rpm}$ within about $5\,\mathrm{s}$. However, no detailed information about the nozzle system is given.

Various parameters of the nozzle design have been elaborated by Rodgers [7] who investigated a turbine impingement with different nozzle design Mach numbers to optimize the start-up performance of a small gas turbine. Also, an impingement compressor impeller was tested. However, only the influence of different nozzle counts and the pressure level was tested on the compressor whereas the design Mach number of 2.3 remained constant.

Over the last years, a quick-start system (QSS) with compressor impeller impingement has been developed and tested successfully on an *Allison 250-C20B* engine in a testbed environment of the Technical University of Munich (TUM) [8]. However, one main drawback for future application in a helicopter is the weight of the system, $46\,\mathrm{kg}$, as proposed by Kerler *et al*. [9]. The pressurized air for the QSS needs to be carried by the rotorcraft in a reservoir during its mission. Therefore, the weight of the QSS is of great importance because it reduces the fuel-saving potential of the single-engine operation strategy. Air consumption has been identified as a significant component for a weight improvement since the pressurized air reservoir takes almost $30\,\%$ of the overall weight of the QSS.

The QSS was initially being designed to use five supersonic nozzles. Since a change of the air supply from the shop air system to a high-pressure bottle it has only operated with three nozzles. Consequently, the nozzles' mass flow rate had to be increased by setting a higher inlet pressure to achieve sufficient acceleration torque on the compressor rotor. However, the supersonic nozzles are operated at pressures higher than the design level at under-expanded exit conditions, reducing their effectiveness and efficiency [10]. In addition to this effect, the overpressure in the impeller section causes a backflow through the compressor. A redesign of the impingement system with adjustment of the nozzles' operating point could reduce the amount of impingement air further.

Since only few information is available from literature, it was decided to carry out a study in which the design parameters of the nozzles and their integration in the impeller casing are investigated. The goal of the investigation presented in this paper is to vary the independent design parameters in a reasonable range. This leads to a prediction model which then can be used for the design process of a new nozzle system. This paper elaborates the process of getting reliable test data starting from an analytical description of the performance of the impingement system. Design of Experiments (DOE) will be used to generate these experimental data on a prototype test rig.

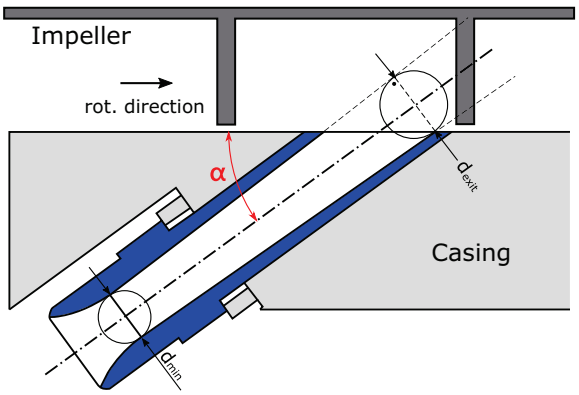

FIG 1. Circumferential cut and installation angle

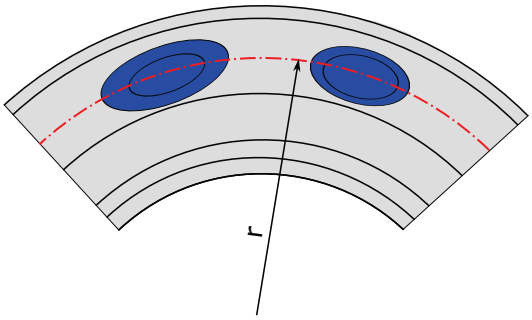

FIG 2. Section of the impeller casing with installation radius

2. EXPERIMENTAL METHODS AND SETUP

In this section the methods for the generation of the test plans are described. Furthermore, the used testing equipment is presented.

2.1. Generation of the test plan

DOE is a statistical tool that helps to investigate the effects of two or more input variables on one or multiple output variables, also called factors and responses [11]. The method offers a systematic approach for designing test plans to reduce the effort and time for running experiments. At the same time, the level of information is kept at a maximum. It also allows increasing the confidence in the results by comparing the significance and random errors of the data. In this study, DOE is used to evaluate the design parameters of the impingement system.

Input variables had to be identified first to derive a test plan for the evaluation of the system. This was done by considering the analytical calculation of the force exerted from a jet on a moving inclined plate as an analogy to the impeller impingement system. Figure 1 shows a cut view through the nozzle installation in the impeller casing at the installation radius (red line in Fig. 2). It illustrates the impingement of a nozzle jet on the outer section of the impeller vanes and the moving direction of the flow passages.

According to Eqn. 1, the ideal impingement force, which is the product of mass flow rate and nozzle exit velocity, is influenced by the installation angle α between the jet and the plate surface and the moving velocity of the plate [12].

$$F_{imp,id} = F_{ex} \cdot \cos\alpha = \dot{m}\left(v_{ex}\ \cos\alpha - v_{plate}\right) \tag{1}$$

$$= \dot{m}\left(\mathrm{Ma}_{ex}\sqrt{\kappa\, R\, T_{ex}}\ \cos\alpha - v_{plate}\right) \tag{2}$$

Rewriting the impulse force of the nozzle jet as a function of the nozzle mass flow rate $\dot{m}$ and the nozzle exit Mach number leads to Eqn. 2 as an expression for the ideal impingement force of a nozzle. Since pressures of up to $50\,\mathrm{bar}$ were used in the experiments, the air was not assumed as an ideal gas but methods proposed by Lemmon *et al.* [13] were used to calculate the thermophysical properties. The results for the gas properties show good agreement with the data tables given in the appendix of the cited publication. The mass flow rate in the critical section of the nozzle was calculated using correlations for the nozzle discharge coefficients depending on the Reynolds number and the gas properties [14] (see Eqn. 3 and Eqn. 4). The nozzle discharge coefficient C_d accounts for three-dimensional effects in the nozzle, reducing the mass flow rate compared with the isentropic calculation.

$$\dot{m}_{red,crit} = \frac{2\,\gamma}{\gamma+1}^{-\frac{\gamma+1}{2(\gamma-1)}} \tag{3}$$

$$\dot{m} = C_d \cdot \dot{m}_{red,crit} \cdot A_{th} \cdot p_{t,th} \cdot \sqrt{Z\,R\,T_{t,th}}^{-1} \tag{4}$$

The results for the discharge coefficient show good agreement compared to experimental results by Kerler *et al.* [15] who determined the mass flow rate with a Coriolis sensor and calculated the discharge coefficient assuming air as an ideal gas. In his publication, a nozzle with a design Mach number of $\mathrm{Ma} = 2.3$ and a throat diameter of $6.6\,\mathrm{mm}$ had been used at pressures up to $18\,\mathrm{bar}$.

Since the impeller flow channels, in which the nozzles impinge, have a strongly three-dimensional character, the two-dimensional assumption of an inclined flat plate is not valid without any restrictions. The unknown effects cannot be calculated analytically and, therefore, are combined in the impingement efficiency η, which is a measure for the amount of the ideally calculated jet momentum that can be transferred to the rotor blades. According to Eqn. 5, the acceleration torque on the gas generator shaft τ results from the effective force acting at the radius r of the impeller as shown in Fig. 2. The impingement efficiency η is defined as the ratio between effective impingement force $F_{imp,eff}$ and ideal force $F_{imp,id}$ which corresponds to the ratio of the measured torque and the torque calculated with the ideal impingement force.

$$\tau = F_{imp,eff} \cdot r \tag{5}$$

$$\eta = \frac{F_{imp,eff}}{F_{imp,id}} = \frac{\tau}{F_{imp,id}\, r} \tag{6}$$

Evaluating the equations, the following variables are identified to influence the torque:

- installation radius r
- installation angle α
- nozzle mass $\dot{m}$ flow as a product of throat area A_{th} and total nozzle inlet pressure $p_{t,in}$
- nozzle exit Mach number Ma_{ex}

The radius will not be further considered because it is evident that maximizing the radius increases torque, and there are no drawbacks from this. The throat area and the absolute value of the inlet pressure are not of interest since they just scale the mass flow rate without any other impact. The influence of the installation angle seems to be evident from Eqn. 1 but as already mentioned the geometric conditions are not identical. Therefore, it is assumed to have a different impact on the torque. The design Mach number appears very interesting because the formation of shock waves can have effects different from the purely linear ones, resulting from Eqn. 2. According to nozzle theory, also the nozzle pressure ratio, i.e. the ratio between the pressure at the nozzle inlet and the exit will influence the efficiency because a nozzle would deliver less thrust if it was under- or over-expanded. The pressure ratio is only dependent on the ratio between inlet pressure and design pressure at constant ambient conditions.

From this analysis, the installation angle, the nozzle Mach number and the pressure level result as input variables for the parametric study. A central composite design (CCD) is used to achieve the capability to detect non-linear effects. Compared to a full-fractional plan, this approach allows the reduction of the number of experiments while almost the same information quality is achieved. Instead of a conventional CCD, where the factors are evaluated at five different levels, a face-centred design was used with three levels for each factor.

In Tab. 1 the chosen factor levels are listed. According to Eqn. 1, the decision for the angles was based on possible geometric solutions, and that angles of more than $45\,\mathrm{deg}$ don't make sense due to expected low impingement force. For the Mach number, the goal was to examine the design space around the existing nozzle system ($\mathrm{Ma} = 2.3$) and to higher levels. Higher values than $\mathrm{Ma} = 3.0$ are not suitable for the application in the QSS because it requires pressures of more than $50\,\mathrm{bar}$ to operate the nozzles in the adapted condition. The reasonable range for the pressure level was decided to be $\pm 30\,\%$ around the design pressure based on experimental data from the QSS and the testbed engine.

TAB 1. Factor levels for DOE

Parameter	Unit	$-$	0	$+$
Angle (A)	$[\mathrm{deg}]$	25	35	45
Mach (M)	$[-]$	2.0	2.5	3.0
Pressure (P)	$[p_t/p_{des}]$	0.7	1.0	1.3

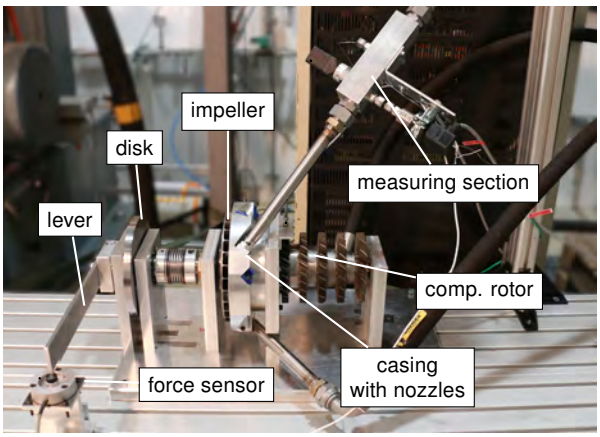

FIG 3. Test Setup

2.2. Test Setup

For the experiments, the original compressor rotor of an *Allison 250-C20B* engine is used. Due to the geometry of the prototype impeller casing, it is not possible to integrate the casing with the stator rows of the 6-stage axial compressor. The rotor is mounted on the surface of the test rig, using two bearing units as depicted in Fig. 3. The end of the rotor shaft (here on the left) is connected to a second shaft that features a disk to have higher inertia. This configuration enables a higher quality of the test data because without the disk, the shaft would accelerate too quickly. The shaft speed is measured with an inductive rotational speed sensor which detects the passing blades of one of the axial wheels. A lever can be attached at the end of the disk shaft to block the rotor and transmit the torque on a force sensor. The measuring section upstream of the nozzle inlet features sensors for static and total pressure and one type K thermocouple for temperature measurement.

For an experiment, three nozzles of the same Mach number are mounted with the same installation angle. Figure 4 shows a close-up of the impeller outlet where a nozzle is installed at an angle of $25\,\mathrm{deg}$. From Fig. 1 it can be seen that cutting the nozzle exit at different angles will change the initially straight nozzle exit diameter d_{ex}. Previous numerical and experimental studies revealed that the slanted nozzles have the same exit Mach number and thrust as the straight nozzles [15]. The throat area of the nozzles is designed to deliver a mass flow rate of $\dot{m} = 0.100\,\mathrm{kg/s}$ at the corresponding design pressure. The nozzles feature a conical shaped divergent section with a half-angle between $2.4\,\mathrm{deg}$ to $4.5\,\mathrm{deg}$ depending on the design Mach number. Having a shorter and optimized nozzle shape is not of interest because the thickness of the casing determines the length of the nozzle. The influence of a nozzle with an optimum shape designed with the Method of Characteristics showed only minor benefits in simulations whereas manufacturing cost would be much higher. The wall of the convergent section has a circular shape and the radius was chosen to achieve a half-angle of $15\,\mathrm{deg}$ at the inlet.

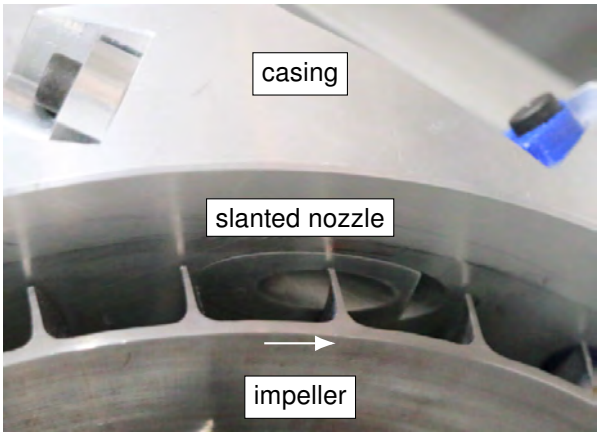

FIG 4. Impeller outlet

The nozzles are supplied with pressurized air from the air supply of the QSS. It is fed from a 300 bar pressure reservoir that allows holding a constant level on the inlet of the spring-loaded pressure regulator. For the static experiments, the impingement system is switched on for 3 s to 4 s . Data samples for the evaluation interval of 1 s are taken with a sampling frequency of 500 Hz towards the end of the test to have settled flow conditions.

2.3. Measurement Uncertainties and Reproducibility

For the experiments carried out in the scope of this work, the pressure setting of the regulator must be set manually. Therefore, it is a source of variance for the test results. The influence of variances of the settings and the performance parameters have been examined as depicted in Tab. 2 to achieve a rating for the quality and robustness of the results.
The available test data of the repetitions of the center point have been evaluated for static and dynamic experiments. The results show that the nozzle inlet pressure varies with a standard variation of $\sigma(\bar{q}) = \pm 0.12$ bar around the mean value of $\mu = 18.67$ bar. The maximum deviations of all ten repetitions lie within an interval from 18.49 bar to 18.90 bar. The setting has good repeatability, with a measurement uncertainty that is $u(q) = 0.24$ bar or 1.30 % based on a single sample. The 95 %-confidence interval around the mean value, is similar to the maximum deviations.
The reproducibility interval for all following quantities lies well in between the measurement uncertainties. For the calculation of absolute and specific torque, the measured force of the lever is used. Due to the highly transient process, the force measurement signal shows significant fluctuations and has a relative measurement uncertainty of $u(q) = 3.8\,\%$. Due to the laws of error propagation, the uncertainties of absolute and specific torque have similar values of 3.8 % respectively 4.1 %. The acceleration time is measured with an accuracy of 1.2 %. This accuracy results from the sampling frequency of the data acquisition system and the uncertainty of the rotor speed measurement of 1.2 % at 10,000 rpm. This results in an accuracy of 3.9 % for the impinged air mass, calculated from the acceleration time and the impingement mass flow.
The significance of the uncertainty effects is addressed by using an ANOVA (ANalysis Of VAriance) table. The total variance of the experiments is split into different contributing factors. Based on the F-test, the p-value is calculated, representing the probability that the obtained result is accurate based on the null hypothesis. Effects are only considered to be significant if the p-value is lower than 0.05. [11]

3. RESULTS OF THE PARAMETRIC ANALYSIS

The test plan was performed in two different configurations in order to distinguish stationary and transient effects. At first, the rotor was fixed, further referred to as “static experiments”. In this setup, the rotor torque generated by the impinging air was measured to evaluate the efficiency of the momentum exchange between the nozzle flow and the rotor. In the second configuration, the “acceleration experiments”, the compressor rotor is spun up to the desired target speed and the time is measured as the most important performance parameter.

3.1. Static Experiments

For the static experiments, the examined output variables are the static impingement efficiency η_{stat} and the so-called *specific torque*. The specific torque corresponds to the specific impulse since it is calculated from the measured rotor torque τ, which is divided by the mass flow rate. It thus helps to erase differences in the mass flow rate due to inaccuracies of the critical nozzle section (manufacturing) and experiment setting (pressure) and compare experiments at different pressure levels. Both, the specific torque and η_{stat}, are a measure for the energy transfer efficiency from the jet to the rotor. However, the difference is that the impingement efficiency η_{stat} takes into account which portion of the jet energy is transferable (see Eqn. 6). In contrast, the specific torque is a quantity to rate the usage efficiency of the air.
Figure 5 depicts the main effect plot for the impingement efficiency. The subplot for the effect of the installation angle is shown but according to the ANOVA results, the factor has no significant influence on the output. After eliminating the non-significant effects, the second ANOVA iteration revealed that the only significant effect is the one of the Mach number as it can also be seen from the plots. The impingement efficiency increases linearly with the Mach number and the difference between the highest and lowest level is around 15 %. This means that for higher Mach numbers, more of the energy in the fluid can be transferred to the rotor.
In Fig. 6, the effects of the factors on the specific torque are shown. The values are depicted relative to the mean value of the repetitions of the central point

TAB 2. Reproducability and repeatability of experiment settings and output variables

Parameter	Unit	$\bar{q}$	$\sigma(q)$	$u(q)$	$\sigma(\bar{q})$	$u(\bar{q})$	
Nozzle Pressure	[bar]	18.67	0.12	0.24	0.12	0.22	1.3 %
Specific Torque	[J/kg]	28.04	0.60	1.17	0.10	0.25	0.9 %
Impingement Eff.	[-]	0.7495	0.0131	0.0257	0.0006	0.0016	0.2 %
Time	[s]	1.428	0.009	0.017	0.008	0.020	1.4 %
Air Mass	[kg]	0.453	0.005	0.009	0.002	0.006	1.3 %

of the test plan ($A = 0$, $M = 0$, $P = 0$) which corresponds to an absolute torque of 8.7 N m. The highest absolute torque of 14.3 N m was achieved with the combination $(-++)$ and the lowest with the combination ($+--$, 4.4 N m). According to ANOVA, only the angle and the Mach number have significant effects which are almost linear. The effect of the Mach number is more dominant than the installation angle. The specific torque at the $\mathrm{Ma} = 3.0$ level is 150 % of the torque at the $\mathrm{Ma} = 2.5$ level which is the same as one would expect from the analytical model. The medium level is closer to $\mathrm{Ma} = 3.0$ than to $\mathrm{Ma} = 2.0$. This observation corresponds to the analytical model. The Mach number has a proportional effect on the nozzle exit velocity and therefore the force on the impeller. At the same time, the static temperature of the nozzle jet decreases which lowers the flow velocity at the outlet if the same total temperature at the nozzle inlet is assumed (see Eqn. 2). However the proportions of the observed effects do not match with the predictions: the flow velocity at $\mathrm{Ma} = 2.0$ should be 10 % lower than $\mathrm{Ma} = 2.5$, but the observed difference of the torque is 22 %, and $\mathrm{Ma} = 3.0$ should be 8 % higher whereas the observed difference is 16 %.

The differences between the levels of the installation angle show good agreement with the differences of the cosine of the corresponding angle. The difference in the influence of the installation angle on the impingement efficiency and the specific torque can be explained by the definitions of the parameters. The impingement efficiency considers the cosine of the installation angle but the specific torque only evaluates how much energy can be transferred at a given mass flow rate.

These results are interesting because they give an idea of how good the analytical model matches reality. Since the installation angle and the Mach number are considered in the impingement efficiency, there should be no effect for the two factors. This is confirmed for the installation angle by the results in Fig. 5. However, the Mach number seems to have influences that the model does not cover. The results of the specific torque rates the performance without taking into account the geometric and fluid mechanical differences. Both output variables don't show a dependency on the pressure level. This is an unexpected result because according to nozzle theory, the maximum efficiency should be achieved at the design pressure level and should be lower in the under- and over-expanded condition [10].

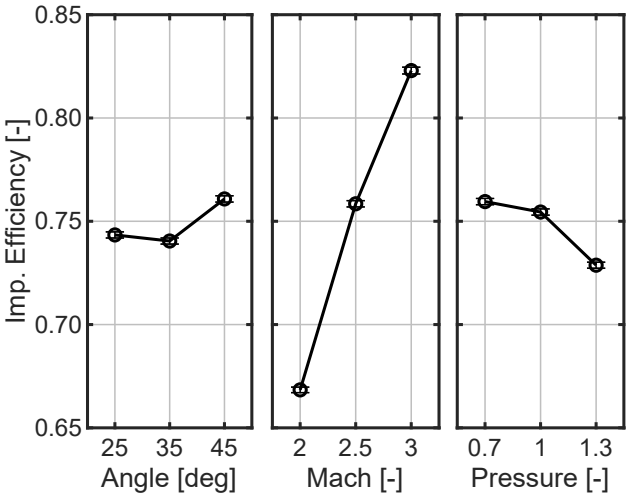

FIG 5. Main effect plot of η_{stat}

3.2. Acceleration Experiments

In the engine application, the QSS is active until the engine has been accelerated to its idling speed of 30,000 rpm. This process takes about 3 s with the help of the electric starter motor and the gas generator turbine which strongly contributes after combustion chamber ignition. With the here used test setup, the target speed for the acceleration experiments was limited to 10,000 rpm. The impingement efficiency η_{acc} of the accelerating rotor was determined by the angular acceleration and the known inertia of the setup. Since the impingement efficiency changes with an increasing rotational speed of the compressor, a mean value was calculated from a sampling interval at the end of the acceleration process close to the target speed of 10,000 rpm. The acceleration time was used to assess the performance of the impingement system. Similar to the characteristic of the specific torque, differences in the mass flow rate influence this parameter. Therefore the achieved acceleration time was corrected by the ratio of the measured mass flow rate and the design rate of 0.100 kg/s per nozzle. This correction is justified by the proportional contribution of the mass flow rate to the nozzle thrust (see Eqn. 4). As another performance parameter, the impinged air mass necessary to accelerate the rotor to the target speed is evaluated.

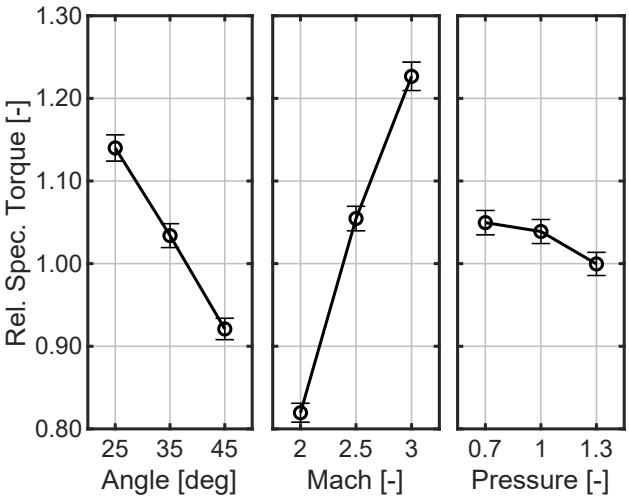

FIG 6. Main effect plot of specific torque

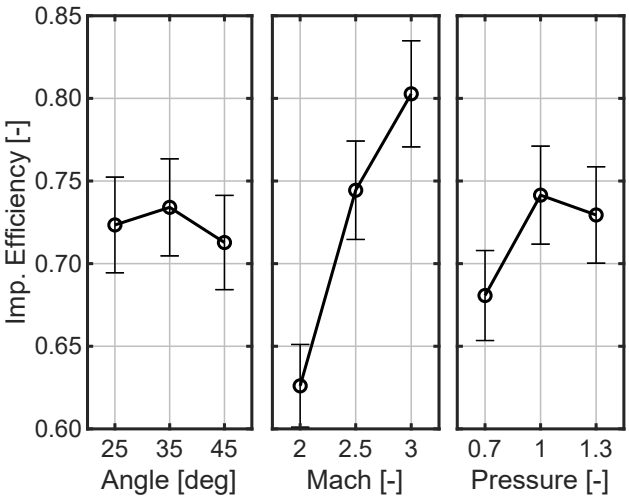

FIG 8. Main effect plot of η_{acc}

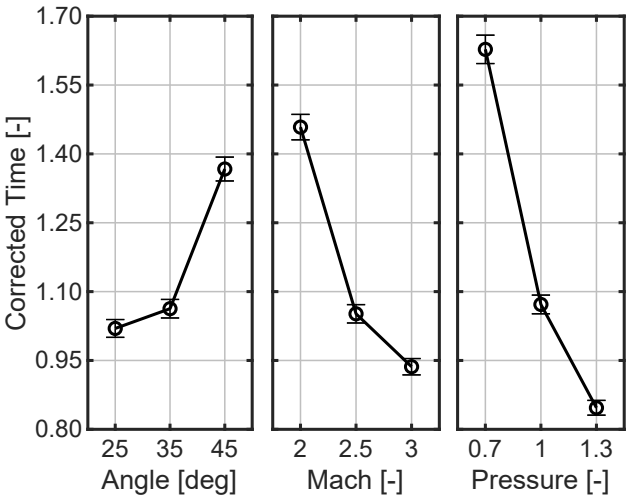

FIG 7. Main effect plot of time

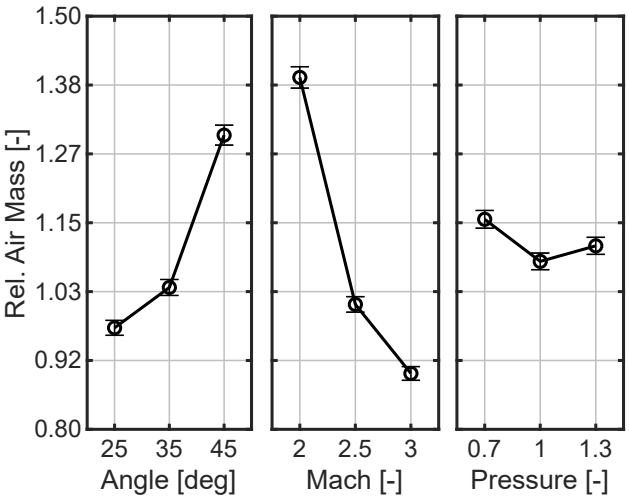

FIG 9. Main effect plot of air mass

Figure 7 shows that all three factors have a significant effect on the acceleration time. Following the results of the specific torque, the acceleration time decreases with decreasing angle and higher Mach number. The pressure level changes the mass flow rate of the system and therefore has a strong effect on the acceleration time. Compared to the plots of the specific torque in Fig. 6, the effects are less linear. This could be an effect of differences in the mass flow rate, which should have been erased by the applied correction or due to the nature of the CCD design, which might overemphasize the central point. The form of the effect plot of the Mach number correlates with the one of the impingement efficiency in Fig. 8, which is a case for the assumption that the time plot has no errors.

The main effect plot of η_{acc} in Fig. 8 shows what is also visible from the ANOVA results: the pressure level and the installation angle do not affect the impingement efficiency. The influence of the Mach number is similar to the static experiments but the plot tends to be less linear since the difference between middle and high level is smaller than between middle and lower level. The plot is similar to the static experiments, although the accuracy of the data is lower due to the transient process and the calculation process of the accelerating torque. The level of the impingement efficiency is about $5\,\%$ lower than in the static setup. Here, the pressure level has no significant effect. However, a slight tendency towards lower efficiency on the lower pressure level can be seen. This underlines that the benefit in acceleration time due to the pressure level is due to the increased mass flow rate and not due to other effects.

The plot of the air mass in Fig. 9 is similar to the results of the specific torque: less air is needed at high Mach numbers and low installation angles. The curves of angle and Mach number look similar to the time plots because the mass flow rate is constant, and the air mass, therefore, scales with the acceleration time.

In addition to the DOE test plan, where the acceleration was limited to $10{,}000\,\mathrm{rpm}$, a series of experiments was conducted where the rotor was accelerated to $20{,}000\,\mathrm{rpm}$. The experiment was only done at an installation angle of $25\,\mathrm{deg}$ since it was the preferred setting after the evaluation of the DOE. The pressure level was kept at design conditions ($p_t/p_{des} = 1.0$).

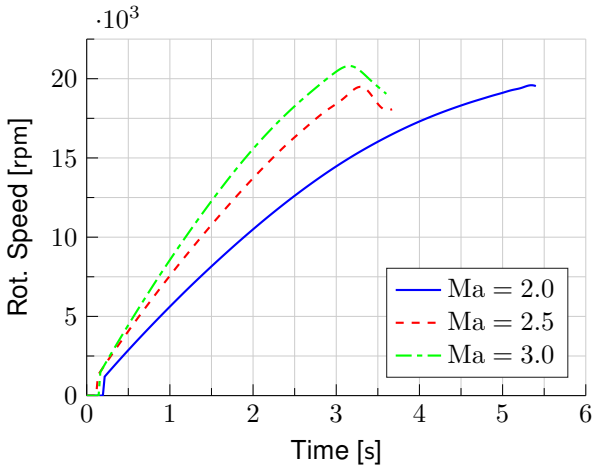

FIG 10. Acceleration to 20,000 rpm

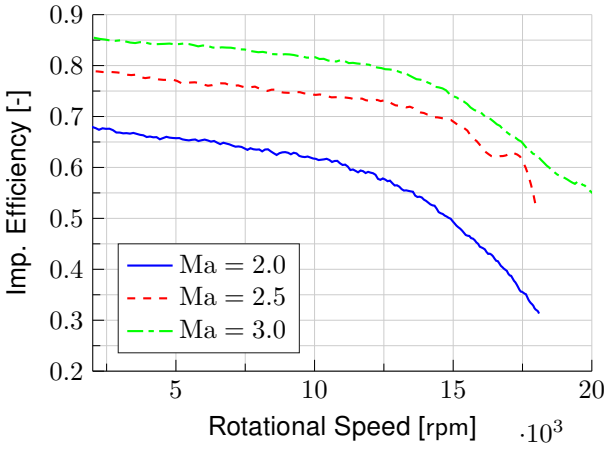

FIG 11. η_{acc} at high rotational speeds

Figure 10 shows the acceleration process over time. As expected, the acceleration of the shaft increases with a higher Mach number. It is visible that for the configuration with a Mach number of $\mathrm{Ma} = 2.0$ a speed of 20,000 rpm is almost the maximum indicated by the flattening curve whereas with $\mathrm{Ma} = 2.5$ and $\mathrm{Ma} = 3.0$ there is still some potential for further acceleration. The plot also shows that the difference between $\mathrm{Ma} = 2.0$ and $\mathrm{Ma} = 2.5$ is the same as between $\mathrm{Ma} = 2.5$ and $\mathrm{Ma} = 3.0$. This is not the same relationship as already known from the time plot in Fig. 7. The time was adjusted with the same linear correction to consider differences in the mass flow rate. Within the first second of the experiments, the acceleration is relatively constant (linear speed curve) but then decreases which can be seen by the flattening curves. This is due to the increased speed of the rotor, which reduces the relative velocity between the nozzle jet and the impeller and therefore lowers the force on the impeller vanes (see Eqn. 2). For $\mathrm{Ma} = 2.0$, this effect is more substantial than for the other two Mach numbers. This observation corresponds to the results of the torque and the acceleration time of the previously discussed experiments.

In Fig. 11 the impingement efficiency is plotted over the rotational speed. The values at low speeds are close to the static impingement efficiency which validates the calculation method. According to Eqn. 1 and Eqn. 6, the calculation of η_{acc} takes into account, that the relative velocity between nozzle jet and impeller vane decreases,. However, all three curves of the plot show a decrease in the efficiency with increasing speed, but it should be constant if there were no other effects. Up to 12,500 rpm, the decrease is linear but then starts to grow rapidly, pushing the efficiency of $\mathrm{Ma} = 2.0$ down to 32 % which is less than half of the static impingement efficiency. This stronger decrease can be observed for all three Mach numbers but is more substantial for $\mathrm{Ma} = 2.0$ than for the other two where the effect is almost equal.

3.3. Discussion of the results

In general, the results show good agreement with the equations presented in section 2 since the trend of the effects corresponds to the analytical predictions. However, some differences have been observed. The influence of the pressure level is not as expected in the static experiments and even disappears when the rotor is accelerated. The reason for this might be that the nozzle jet interacts with the passing impeller vanes which then changes the flow conditions and the formation of shock and expansion waves. The effect of the Mach number on the static impingement efficiency is a second indication for this thesis. An examination of the flow field in the region of the nozzle exits was not possible with the available test setup. Still, earlier studies tried to investigate the flow conditions by conducting Schlieren photography on a simplified model of the impingement situation [16]. It was discovered that the formation of shock and expansion waves changes with alternating pressure, but the energy transfer impact was not examined. The results from the static experiments and the acceleration to 10,000 rpm suggest that the pressure level has no influence on the performance of the impingement system. However, the results from the acceleration to 20,000 rpm show a different picture. The strong decrease of the impingement efficiency is most likely caused by the increased exit pressure of the rotor at high rotational speeds.
For the application in the engine, the performance of the impingement system at different pressure levels is an important characteristic since the pressure at the compressor outlet changes from atmospheric pressure to a pressure ratio of about 2:1 during the ground idle starting procedure.
Another aspect to take into account is that the compressor experiences reverse flow during the impingement process. This happens because the compressor flow is disturbed by the impingement flow and can't work against the positive pressure gradient caused by the stagnation of the impingement air in the compressor volume and the pressure in the combustion chamber [17]. If the nozzle was operated

in an over-expanded condition and with a lower mass flow rate, less reverse flow through the compressor would occur. The reverse flow is counteractive in a single-stage radial compressor because it then works as a brake and reduces acceleration [7]. In the here regarded compressor, the effect is more severe due to the six axial compressor stages in front of the radial end-stage and can even result in compressor stall and surge [17]. Operation in the over-expanded condition therefore would be beneficial. Still, the results of this study indicate that there is a negative influence of a lower pressure level, although it had no significant effect on the evaluation parameters.
The differences between the performance parameters of static and acceleration experiments conclude that in the here regarded case, effects are present which are not covered by the analytical description. A study by Rodgers [7] had used an impeller with similar velocity coefficients, but different results where discovered. One possible reason for these differences could be the geometric proportions since the here regarded compressor has smaller flow channels.
The experiments confirmed the influence of the nozzle installation angle that was expected from the analytical results. There was no sign of any other effects that could improve the performance of higher angles compared to smaller ones. It should therefore be tried to make the installation angle as small as possible within the geometric limitations. For the *Allison 250-C20B* the minimum angle with the current design of the impingement air supply is $25\,\mathrm{deg}$ since some space is needed for the supply pipes around the compressor casing. Therefore, there is no change compared to the initial configuration by Hönle [8] is proposed.
The Mach number has been revealed to be the most promising parameter to improve performance of the impingement system. Static and acceleration experiments have shown that the impinged air mass can be used more effectively and more efficiently at higher Mach numbers. There are no disadvantages of higher Mach numbers in performance (acceleration and impinged air mass). The performance improvement from $\mathrm{Ma} = 2.0$ to $\mathrm{Ma} = 2.5$ is significantly bigger than from $\mathrm{Ma} = 2.5$ to $\mathrm{Ma} = 3.0$. For the application in the engine, it must be taken into consideration that higher Mach numbers also require higher nozzle inlet pressures which increases with the square root of the Mach number. The impingement system of the engine uses an air tank with a pressure of $300\,\mathrm{bar}$ to store the required air in a small volume. The air is then expanded to the required pressure with a regulator. For lower Mach numbers more of the fluid's energy is dissipated in the regulator valve. The piping system behind the regulator must be designed adequately for the required pressure but more importantly the air reservoir loses parts of its potential at higher nozzle pressures. A Mach number of $\mathrm{Ma} = 3.0$ requires a pressure ratio of 36.8 whereas for $\mathrm{Ma} = 2.0$ only 7.8 is needed. This difference means that almost $10\,\%$ of the air stored in the reservoir can't be used at $\mathrm{Ma} = 3.0$. Consequently, an increase of the design Mach number must lower the used air mass by the amount of lost potential of the air reservoir.

TAB 3. Results of the prediction models

Mach	Pressure	Air [kg]	Time [s]
2.3	12.5	1.092	3.33
2.5	17.1	0.932	2.80
2.6	20.0	0.873	2.71
2.7	23.3	0.828	2.59
2.8	27.2	0.796	2.50
3.0	36.8	0.777	2.46

In order to support the design decision for a new version of the impingement system, prediction models were derived from the results of the acceleration experiments to $20{,}000\,\mathrm{rpm}$. The results are shown in Tab. 3. The benefits of higher Mach numbers in acceleration time and air consumption were compared to the drawback in usable air volume. The analysis revealed that the range of $\mathrm{Ma} = 2.6$ to $\mathrm{Ma} = 2.8$ is the preferable choice. In comparison with the currently used nozzles that have a design Mach number of $\mathrm{Ma} = 2.3$, a nozzle with $\mathrm{Ma} = 2.7$ offers $24\,\%$ less air consumption and a $22\,\%$ shorter acceleration time.

4. CONCLUSIONS AND OUTLOOK

In this study, an experimental investigation on a radial compressor impingement system that can be used to reduce the run-up time of a gas turbine engine has been carried out. A systematic approach using DOE for the design and evaluation of the test plan was presented. The effect of the three chosen input variables installation angle, nozzle design Mach number and pressure level was examined within a reasonable range for a later redesign of the impingement system which is adapted for an *Allison 250-C20B* testbed engine. Measures for the efficiency of the impingement, the generated torque on the impeller rotor, the used air mass and the time needed to accelerate to a specific target speed were chosen as output variables. The results show, that the pressure level has no significant impact on the impingement system's efficiency and performance. The effect of the installation angle strictly follows the proportions that can be assessed from analytical calculations. Also the Mach number has an important influence on efficiency and performance. The results in the investigated range between Mach numbers from $\mathrm{Ma} = 2.0$ to 3.0 suggest that there might be a peak in the achievable run-up time at higher Mach numbers. However, extrapolation of the effects is not permitted with the applied DOE methods. For the static experiments, the effects of the Mach number were rather linear whereas in the acceleration experiments they became more non-linear. This is a sign for effects that are not described by the

analytical model and might be caused by the interaction of the moving impeller vanes and the nozzle jet.
For the application in the engine, not only the acceleration time and the used air mass is of importance. Also the necessary air supply pressure is of high importance. The pressure influences the weight of the tubing and the amount of air stored in the reservoir that can be used. Therefore, the range of Mach numbers with the best performance ($\mathrm{Ma} = 2.5$ to $\mathrm{Ma} = 3.0$) was compared to the currently used impingement system which uses nozzle with a design Mach number of $\mathrm{Ma} = 2.3$. The range from $\mathrm{Ma} = 2.6$ to $\mathrm{Ma} = 2.8$ is the preferred range for a redesign of the impingement system of the engine. The required pressure is still at a moderate level while the performance in terms of impingement air and acceleration time is close to the maximum at $\mathrm{Ma} = 3.0$ With a design Mach number of $\mathrm{Ma} = 2.7$ the improvement in acceleration time and used air could be as high as $24\,\%$ respectively $22\,\%$ compared to the current system.
The results gained from this investigation show the benefits of a redesign of the current impingement system. However, some improvements are proposed for future experiments. The used test setup is close to the real engine in terms of inertia of the rotor but it has not been possible to include the axial compressor casing. The compressor casing would have two effects that both result in slower acceleration: First, the stator vanes would allow a pressure rise across the axial compressor which means that the consumed power increases. Second, any reverse flow caused by the impingement air flow would apply a decelerating torque on the rotor. Furthermore, the test setup offers no possibility to throttle the compressor arrangement which would influence the pressure level at the nozzle exit and the power consumed by the compressor. Future studies will include these components to adjust the test setup conditions to those of the real conditions in the engine. A new impingement system was designed with a nozzle Mach number of $\mathrm{Ma} = 2.7$ and is already integrated into the engine. Experiments will be carried out to compare the results to those made in this publication and to the performance of the old engine system.

Acknowledgements

The authors want to thank their colleague Marcel Schmieder (TUM) for the provision his MATLAB class for the calculation of real air gas properties considering the methods of Lemmon *et al.* [13].
This work is supported by the “QuickStart” project (funding number 20E1727) through the German National Aerospace Research Program (Lufo V-3).

References

[1] A. Garve. Arrangements for Radial Flow Compressors for Supercharging Internal Combustion Engines. Technical report, Maschinenfabrik Augsburg-Nürnberg AG, 1969. *US Patent No. 3,462,071.* Washington, DC: United States Patent and Trademark Office.

[2] J. Schröder, H.-G. Bozung, R. Bandel, and H. Mendle. Turbo Supercharger for an Internal Combustion Engine. Technical report, M.A.N. - B&W Diesel GmbH, 1987. *US Patent No. 4,689,960.* Washington, DC: United States Patent and Trademark Office.

[3] D. W. Legg. Air Start/Assist for Turbochargers. Technical report, Cameron International Corp., 1993. *US Patent No. 5,218,822.* Washington, DC: United States Patent and Trademark Office.

[4] D. Daggett. Tip Impingement Turbine Air Starter for Turbine Engine. Technical report, Boeing Company, 2003. *US Patent Application No. 2003/0131607 A1.* Washington, DC: United States Patent and Trademark Office.

[5] L. J. Veilleux. Lightweight Start System for a Gas Turbine Engine. Technical report, Hamilton Sundstrand Corporation, 2010. *European Patent Application No. 2 267 288 A2.* Munich, Germany: European Patent Office.

[6] A. Jones. Start System for Expandable Gas Turbine. Technical report, Hamilton Sundstrand Corporation, 2005. *US Patent No. 6941760 B1.* Washington, DC: United States Patent and Trademark Office.

[7] C. Rodgers. Impingement Starting and Power Boosting of Small Gas Turbines. *Journal of Engineering for Gas Turbines and Power*, 107(4):821–827, October 1985. DOI: 10.1115/1.3239817.

[8] J. Hönle, A. Barth, W. Erhard, and H.-P. Kau. Engine Quick Start in Case of Emergency - A Requirement for saving Fuel by Means of Engine Shutdown. In *38th European Rotorcraft Forum*, volume 1, pages 434–441, September 2012. Code 97880. DOI: 10.2514/6.2016-5062.

[9] M. Kerler, C. Schäffer, W. Erhard, and V. Gümmer. Design of an Airworthy Turboshaft Engine Quick-Start System with Compact Pressurized Air Supply for Rotorcraft Application. In *42nd European Rotorcraft Forum*, volume 2, pages 1459–1465, September 2016. Code 128734.

[10] J. Délery. *Handbook of Compressible Aerodynamics*. ISTE and John Wiley & Sons, London and Hoboken, NJ, 1. publ edition, 2010. ISBN: 9781848211414.

[11] K. Siebertz, D. van Bebber, and T. Hochkirchen. *Statistische Versuchsplanung: Design of Experiments (DoE)*. VDI-Buch Ser. Vieweg, Berlin, Heidelberg, 2nd ed. edition, 2017. ISBN: 9783662557426.

[12] H. Song. *Engineering Fluid Mechanics*. Metallurgical Industry Press and Springer, Beijing and Singapore, 2018. ISBN: 9789811301735.

[13] E. Lemmon, R. Jacobsen, S. Penoncello, and D. Friend. Thermodynamic Properties of Air and Mixtures of Nitrogen, Argon, and Oxygen From 60 to 2000 K at Pressures to 2000 MPa. *Journal of Physical and Chemical Reference Data*, 29(3), September 2000. DOI: 10.1063/1.1285884.

[14] D. Rist. *Dynamik realer Gase: Grundlagen, Berechnungen und Daten für Thermogasdynamik, Strömungsmechanik und Gastechnik*. Springer Berlin Heidelberg, 1996. ISBN: 9783642648229. DOI: 10.1007/978-3-642-61402-6.

[15] M. Kerler, C. Schäffer, W. Erhard, and V. Gümmer. Design Parameter Identification of the Air Supply for a Turboshaft Engine Quick-Start System. In *52nd AIAA/SAE/ASEE Joint Propulsion Conference*. American Institute of Aeronautics and Astronautics Inc, AIAA, July 2016. AIAA 2016-5062. DOI: 10.2514/6.2016-5062.

[16] A. Barth. *Konstruktion einer Verdichterpralldüse für das Triebwerk Allison 250-C20B*. Student Thesis, Technical University of Munich, Munich, Germany, May 2011.

[17] N. Kuen and V. Gümmer. Experimental Investigation of the Starting Procedure of a Helicopter Gas Turbine Featuring an Impingement Quick-Start System. In *Proceedings of ASME Turbo Expo 2020*, volume 1, pages 434–441, Virtual, Online, September 2020. Code 97880. DOI: 10.1115/GT2020-16231.